

The escape fraction of ionizing photons from high redshift galaxies from data-constrained reionization models

Sourav Mitra^{1*}, Andrea Ferrara^{2†} and T. Roy Choudhury^{3‡}

¹Harish-Chandra Research Institute, Chhatmag Road, Jhusi, Allahabad 211019, India

²Scuola Normale Superiore, Piazza dei Cavalieri 7, 56126 Pisa, Italy

³National Centre for Radio Astrophysics, TIFR, Post Bag 3, Ganeshkhind, Pune 411007, India

21 August 2018

ABSTRACT

The escape fraction, f_{esc} , of ionizing photons from high-redshift galaxies is a key parameter to understand cosmic reionization and star formation history. Yet, in spite of many efforts, it remains largely uncertain. We propose a novel, semi-empirical approach based on a simultaneous match of the most recently determined Luminosity Functions (LF) of galaxies in the redshift range $6 \leq z \leq 10$ with reionization models constrained by a large variety of experimental data. From this procedure we obtain the evolution of the best-fit values of f_{esc} along with their $2\text{-}\sigma$ limits. We find that, averaged over the galaxy population, (i) the escape fraction increases from $f_{\text{esc}} = 0.068^{+0.054}_{-0.047}$ at $z = 6$ to $f_{\text{esc}} = 0.179^{+0.331}_{-0.132}$ at $z = 8$; (ii) at $z = 10$ we can only put a lower limit of $f_{\text{esc}} > 0.146$. Thus, although errors are large, there is an indication of a 2.6 times increase of the average escape fraction from $z = 6$ to $z = 8$ which might partially release the “starving reionization” problem.

Key words: dark ages, reionization, first stars – intergalactic medium – cosmology: theory – large-scale structure of Universe.

1 INTRODUCTION

One of the most crucial issues regarding the evolution of intergalactic medium (IGM) and cosmic reionization is the escape fraction, f_{esc} , of ionizing photons from high-redshift galaxies. This parameter remains poorly constrained in spite of the many theoretical and observational attempts made in past few years. The difficulties largely arise from the lack of a full understanding of the physics of star formation, radiative transfer and feedback processes, and from uncertainties on the properties of the high- z galaxy interstellar medium (ISM); as a result, derived values of f_{esc} span the large range 0.01 – 1 (Fernandez & Shull 2011). Observationally, f_{esc} can be reliably estimated only at redshifts $z \lesssim 3$ (Leitherer et al. 1995; Dove, Shull, & Ferrara 2000; Heckman et al. 2001; Ciardi, Bianchi & Ferrara 2002; Giallongo et al. 2002; Fernández-Soto et al. 2003; Inoue et al. 2005; Bergvall et al. 2006; Shapley et al. 2006; Vanzella et al. 2010). On the other hand, theoretical studies (Wood & Loeb 2000; Razoumov & Sommer-Larsen 2006; Gnedin 2008; Gnedin, Kravtsov & Chen 2008; Srbnovsky & Wyithe 2010; Razoumov & Sommer-Larsen 2010; Yajima, Choi & Nagamine 2011; Haardt & Madau 2011; Fernandez & Shull 2011; Kuhlen & Faucher-Giguere 2012) have been rather inconclu-

sive so far, as illustrated by their often conflicting results in terms of f_{esc} values and trend with redshift and galaxy mass.

One key aspect of reionization lies in its close coupling with the properties and evolution of first luminous sources (for reviews, see Loeb & Barkana 2001; Barkana & Loeb 2001; Choudhury & Ferrara 2006a; Choudhury 2009). Observations of cosmic microwave background (CMB) and highest redshift QSOs put very tight constraints on the reionization history; these allow to construct self-consistent models of structure formation (Choudhury & Ferrara 2005; Wyithe & Loeb 2005; Gallerani, Choudhury & Ferrara 2006; Choudhury & Ferrara 2006b; Dijkstra, Wyithe & Haiman 2007; Samui, Srianand & Subramanian 2007; Iliev et al. 2008; Kulkarni & Choudhury 2011). The most favorable model, which is consistent with the Thomson scattering optical depth $\tau_{\text{e1}} = 0.088 \pm 0.015$ from WMAP7 data (Larson et al. 2010) and the Gunn-Peterson optical depth evolution from QSO absorption line experiments at $z \gtrsim 6$ (Fan et al. 2006), suggests that reionization is an extended process over the redshift range $6 \lesssim z \lesssim 15$ (Choudhury & Ferrara 2006b; Mitra, Choudhury & Ferrara 2011, 2012). This model also indicates that reionization feeds back on star formation by suppressing it in the low-mass haloes at early times (Thoul & Weinberg 1996; Choudhury & Ferrara 2007).

In parallel, direct observations of galaxies at epochs close to the end of reionization have made astonishing progresses over the past few years (Bouwens & Illingworth 2006; Iye et al. 2006; Bouwens et al. 2007, 2008; Ota et al. 2008; Bouwens et al.

* E-mail: smitra@hri.res.in

† E-mail: andrea.ferrara@sns.it

‡ E-mail: tirth@ncra.tifr.res.in

2009; Henry et al. 2009; Bouwens et al. 2010; Oesch et al. 2010; Bouwens et al. 2010; McLure et al. 2010; Oesch et al. 2012; Bradley et al. 2012). allowing to derive the galaxy UV Luminosity Function (LF) up to $z \approx 10$ (Bouwens & Illingworth 2006; Bouwens et al. 2010; Oesch et al. 2012), and to better constrain light production by reionization sources.

Here we aim at combining data-constrained reionization histories and the evolution of the LF of early galaxies to get an empirical determination of the escape fraction. The study also provides relatively tight constraints also on the evolution of the star-forming efficiency ϵ_* (Faucher-Giguère et al 2008a; Kuhlen & Faucher-Giguere 2012). Throughout the paper, we assume a flat Universe with cosmological parameters given by the WMAP7 best-fit values: $\Omega_m = 0.27$, $\Omega_\Lambda = 1 - \Omega_m$, $\Omega_b h^2 = 0.023$, and $h = 0.71$. The parameters defining the linear dark matter power spectrum are $\sigma_8 = 0.81$, $n_s = 0.97$, $dn_s/d \ln k = 0$ (Larson et al. 2010). Unless mentioned, quoted errors are 2σ .

2 DATA-CONSTRAINED REIONIZATION

We start by summarizing the main features of the semi-analytical model used in this work, which is based on Choudhury & Ferrara (2005) and Choudhury & Ferrara (2006b).

The model follows the ionization and thermal histories of neutral, HII and HeIII regions simultaneously also accounting for IGM inhomogeneities described by a lognormal distribution as in Miralda-Escudé, Haehnelt, & Rees (2000). Sources of ionizing radiation are stars and quasars. The stellar sources, all characterized by a Salpeter IMF in the mass range $M_* = 1 - 100 M_\odot$, can be divided into two classes, namely, (i) metal-free (i.e. PopIII) stars; (ii) PopII stars with sub-solar metallicities. The transition is based on a local critical metallicity criterion. Radiative feedback, suppressing star formation in low-mass haloes, is included through a Jeans mass prescription based on the evolution of the thermal properties of the IGM.

Given the collapsed fraction f_{coll} of dark matter haloes, the production rate of ionizing photons in the IGM is

$$\dot{n}_{\text{ph}}(z) = n_b N_{\text{ion}} \frac{df_{\text{coll}}}{dt} \quad (1)$$

where n_b is the IGM number density, and N_{ion} is the number of photons entering the IGM per baryon included into stars. The parameter N_{ion} can actually be written as a combination of three parameters: the star-forming efficiency ϵ_* (fraction of baryons within collapsed halos going into stars), f_{esc} , and the specific number of photons emitted per baryon in stars, N_γ , which depends on the stellar IMF and the corresponding stellar spectrum:

$$N_{\text{ion}} = \epsilon_* f_{\text{esc}} m_p \int_{\nu_{\text{HI}}}^{\infty} d\nu \left[\frac{dN_\nu}{dM_*} \right] = \epsilon_* f_{\text{esc}} N_\gamma \quad (2)$$

In our previous work (Mitra, Choudhury & Ferrara 2011, 2012), we assumed N_{ion} to be an unknown function of z and decompose it into its principal components. The Principal Component Analysis filters out components of the model that are most sensitive to the data and thus most accurately constrained. In the following we assume a single stellar population (PopII) when computing the ionizing radiation properties; any change in the characteristics of these stars over time would be accounted for indirectly by the evolution of N_{ion} . We also include the contribution of quasars at $z < 6$ assuming that they have negligible effects on IGM at higher redshifts; however, they are significant sources of ionizing photons at $z \lesssim 4$.

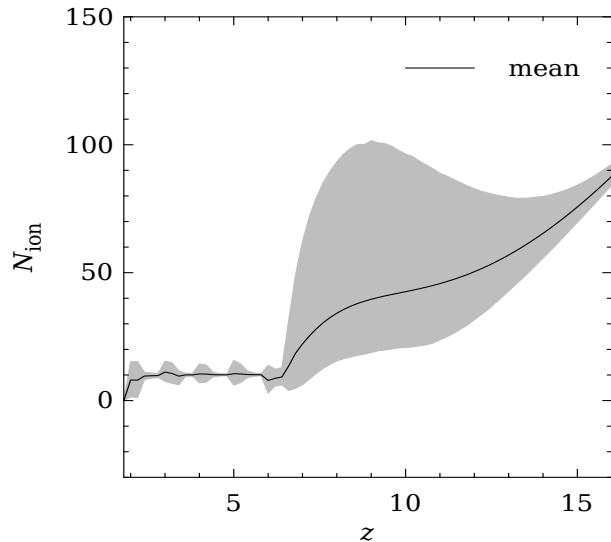


Figure 1. Redshift evolution of N_{ion} obtained from the Principal Component Analysis using WMAP7 data. The solid line corresponds to the model described by mean values of the parameters while the shaded region corresponds to 2σ limits.

From the above model, we obtain the redshift evolution of N_{ion} by doing a detailed likelihood analysis using three different data sets - the photoionization rates Γ_{PI} obtained using Ly α forest Gunn-Peterson optical depth observations and a large set of hydrodynamical simulations (Bolton & Haehnelt 2007), the redshift distribution of Lyman Limit Systems dN_{LL}/dz in $0.36 < z < 6$ (Songaila & Cowie 2010) and the angular power spectra C_l for TT, TE and EE modes using WMAP7 (Larson et al. 2010) and forecasted PLANCK data. We show the redshift evolution of $N_{\text{ion}}(z)$ obtained from our Principal Component Analysis using WMAP7 data in Fig. 1. The solid line corresponds to the model described by mean values of the parameters which we obtained by performing a Monte-Carlo Markov Chain (MCMC) analysis over the parameter space of our model, while the shaded region corresponds to its 2σ limits. We concluded that it is not possible to match available reionization data with a constant N_{ion} over the whole redshift range (Mitra, Choudhury & Ferrara 2011, 2012). Rather, it must increase at $z > 6$ from its constant value at lower redshifts. This is a signature of either a varying IMF and/or evolution in the star-forming efficiency and/or photon escape fraction of galaxies, as eq. 2 clearly shows.

At this point, it is worth pointing out some of the caveats in our formalism based on PCA. The MCMC analysis for this work was done using 2–8 PCA modes (Mitra, Choudhury & Ferrara 2012). Truncating a PCA expansion can reduce the variance in the estimation of the reionization history, but also introduces a bias towards the fiducial history. In order to account for this, we used the Akaike information criteria (AIC) to reduce the intrinsic bias present in any particular choice of fiducial model. We found that at $z \leq 6$, the strong Lyman- α forest constraints essentially fix N_{ion} , so that the efforts to reconstruct the reionization history are very promising at these redshifts. On the other hand, it is much more difficult to recover N_{ion} or the other various quantities related to reionization history at $z > 6$ in a truly model-independent manner as there exists a considerable amount of bias at this high redshift end (Mitra, Choudhury & Ferrara 2011, 2012). It is possible that for these redshifts, the statistical uncertainties may have been hidden as systematic uncertainties (Huterer & Starkman 2003). How-

ever, with more data it would be possible to apply this technique in a regime where the variance in N_{ion} is small enough to produce a useful constraint on the reionization history without the need to truncate the PCA modes so severely and so without introducing any bias. This technique will become more applicable as more data becomes available for $z > 6$ region.

3 LUMINOSITY FUNCTION EVOLUTION

The effect of reionization on the high redshift galaxy LF was studied using the semi-analytical models by Samui, Srianand & Subramanian (2007) and Kulkarni & Choudhury (2011). In this work, we follow their method to study the evolution of LF for our model.

The LF is derived as follows. We compute the luminosity at 1500 Å of a galaxy having the halo mass M and age Δt using

$$L_{1500}(M, \Delta t) = \epsilon_* \left(\frac{\Omega_b}{\Omega_m} \right) M l_{1500}(\Delta t) \quad (3)$$

Here the age of the galaxy formed at z' and observed at z is $\Delta t = t_z - t_{z'}$, $l_{1500}(\Delta t)$ is a template specific luminosity at 1500 Å for the stellar population of age Δt . As we restrict to a single stellar population, i.e. PopII stars, ϵ_* indicates the star forming efficiency of PopII stars throughout the paper.

To compute l_{1500} , we use stellar population models of Bruzual & Charlot (2003) for PopII stars. The UV luminosity depends on galaxy properties including the IMF, star formation rate (SFR), stellar metallicity (Z) and age. Dayal et al. (2009a) and Dayal, Ferrara & Saro (2010) have shown that the metallicity correlates with stellar mass, and the best fit mass-metallicity relation they find is

$$Z/Z_\odot = (0.25 - 0.05\Delta z) \log_{10}(M_*) - (2.0 - 0.3\Delta z) \quad (4)$$

where $\Delta z = (z - 5.7)$ and M_* is the total stellar mass of the galaxy. We take all the available stellar population models in the metallicity range $Z = 0.0001 - 0.05$ for PopII stars and interpolate them to compute l_{1500} following the mass-metallicity relation given by the above relation for our model galaxies.

The luminosity can be converted to a standard absolute AB magnitude (Oke & Gunn 1983; Samui, Srianand & Subramanian 2007; Kulkarni & Choudhury 2011) using

$$M_{AB} = -2.5 \log_{10} \left(\frac{L_{\nu_0}}{\text{erg s}^{-1} \text{Hz}^{-1}} \right) + 51.60 \quad (5)$$

The luminosity function $\Phi(M_{AB}, z)$ at any redshift z is then given by

$$\Phi(M_{AB}, z) = \frac{dn}{dM_{AB}} = \frac{dn}{dL_{1500}} \frac{dL_{1500}}{dM_{AB}}, \quad (6)$$

where

$$\frac{dn}{dL_{1500}} = \int_z^\infty dz' \frac{dM}{dL_{1500}}(L_{1500}, \Delta t) \frac{d^2 n}{dM dz'}(M, z') \quad (7)$$

is the comoving number of objects at redshift z with observed luminosity within $[L_{1500}, L_{1500} + dL_{1500}]$. The quantity $d^2 n/dM dz'$ gives the formation rate of haloes of mass M , which we obtain as in Choudhury & Ferrara (2007). Note that, we can vary the star-forming efficiency ϵ_* in eq. 3, as a free parameter and obtain its best-fit value by comparing the high-redshift LFs computed using the above equations with observations.

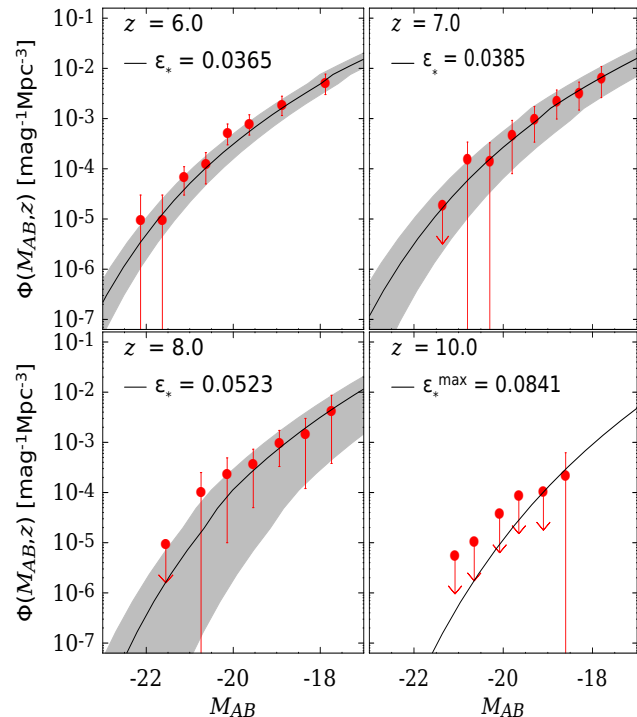


Figure 2. Luminosity function from our model for best-fit ϵ_* (black curve) and its 2- σ limits (shaded region) at $z = 6, 7, 8$ and 10. Data points with 2- σ errors are from Bouwens & Illingworth (2006) ($z = 6$), Bouwens et al. (2010) ($z = 7, 8$) and Oesch et al. (2012) ($z = 10$). For $z = 10$, we show the luminosity function from our model for the maximum value of ϵ_* for which the LF curve does not exceed the experimental upper limits.

3.1 Constraining the escape fraction

Our strategy to constrain f_{esc} exploits the combination between the previously derived (Sec. 2) evolution of N_{ion} , and the constraints on ϵ_* that can be derived from matching LFs at different redshifts. Once the (Salpeter) IMF of the (PopII) stars is fixed, N_γ is also fixed and equal to ≈ 3200 ; from eq. 2 we then get the value of f_{esc} as follows:

$$f_{\text{esc}} = \frac{N_{\text{ion}}}{\epsilon_* N_\gamma} \quad (8)$$

As the uncertainties on $[N_{\text{ion}}/N_\gamma]$ and ϵ_* are independent, the fractional uncertainty in f_{esc} can be obtained from the quadrature method (Taylor 1997), i.e.

$$\frac{\delta f_{\text{esc}}}{f_{\text{esc}}} = \sqrt{\left(\frac{\delta [N_{\text{ion}}/N_\gamma]}{[N_{\text{ion}}/N_\gamma]} \right)^2 + \left(\frac{\delta \epsilon_*}{\epsilon_*} \right)^2} \quad (9)$$

In this work, we are interested in the $z \geq 6$ evolution of the escape fraction. In principle, our approach can also be used for the lower redshift range $3 \leq z \leq 5$, provided that a detailed treatment of dust extinction is added to our model. The underlying assumption in the present work is that dust effects on the escape fraction can be safely neglected at early times.

4 RESULTS

The observationally determined LFs are taken from Bouwens & Illingworth (2006) for $z = 6$, Bouwens et al. (2010) for $z = 7, 8$ and Oesch et al. (2012) for $z = 10$. Figure 2 shows the globally averaged LFs calculated using our model for

Redshift	Best-fit ϵ_*	2- σ limits	Best-fit f_{esc}	2- σ limits
$z = 6$	0.0365	[0.0253, 0.0481]	0.0684	[0.0210, 0.1221]
$z = 7$	0.0385	[0.0193, 0.0576]	0.1607	[0.0319, 0.4451]
$z = 8$	0.0523	[0.0129, 0.0822]	0.1794	[0.0466, 0.5098]
$z = 10$	< 0.0841		> 0.1456	

Table 1. Best-fit values and 2- σ limits of ϵ_* and the derived parameter f_{esc} for the reionization model obtained from the LF calculation at different redshifts. At $z = 10$, we get only an upper limit of ϵ_* and a corresponding lower limit of f_{esc} .

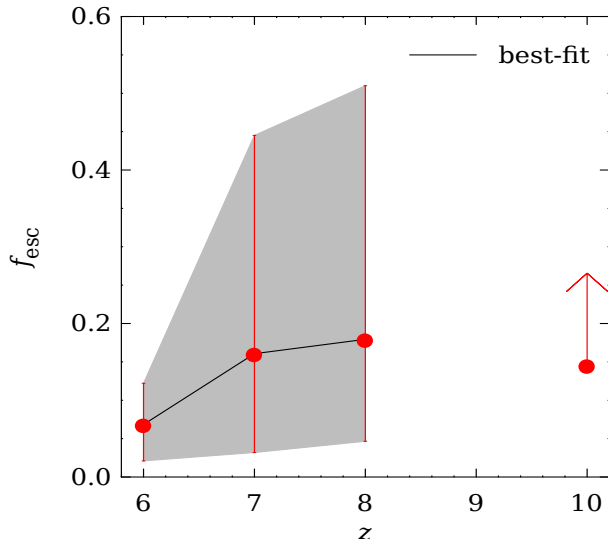


Figure 3. Redshift evolution of the escape fraction f_{esc} with 2- σ errors. The $z = 10$ data point shows the lower limit of f_{esc} . The solid line corresponds to its best-fit value while the shaded region corresponds to 2- σ limits.

$z = 6, 7, 8, 10$ compared to the observational data points. The $z = 10$ data are obtained from the detection of a single galaxy candidate by Oesch et al. (2012); hence, we only show results for the maximum value of ϵ_* for which the LF curve does not exceed the experimental upper limits.

Our model reproduces the observed LFs reasonably well, especially at lower redshifts. From such a match we find that the best-fit value of the star-formation efficiency ϵ_* nominally increases from 3.6% at $z = 6$ to 5.2% at $z = 8$. Such a small variation is statistically consistent with a constant value of ϵ_* , i.e. no evolution.

The corresponding values of f_{esc} calculated using eq. 8 and 9 are plotted in Fig. 3 along with the 2- σ confidence limits (shaded region). The numerical values for ϵ_* and f_{esc} are also reported in Table 1 for different redshifts ($z = 6, 7, 8$). The escape fraction shows a moderately increasing trend from $f_{\text{esc}} = 0.068_{-0.047}^{+0.054}$ at $z = 6$ to $f_{\text{esc}} = 0.179_{-0.132}^{+0.331}$ at $z = 8$; at $z = 10$ we can only put a lower limit of $f_{\text{esc}} > 0.146$, corresponding to the maximum allowed value of $\epsilon_* = 0.0841$.

The reported 2- σ errors are however relatively large and we cannot exclude a non-evolving galaxy-averaged trend for f_{esc} . The uncertainties become larger with redshift as a consequence of the fact that the larger LF errors at higher redshifts.

5 CONCLUSIONS

We have used a semi-analytical model, based on Choudhury & Ferrara (2005) and Choudhury & Ferrara (2006b) to compare the UV luminosity functions at different epochs predicted

from our model with the observed LF to constrain the parameters related to star formation history in the redshift range $6 \leq z \leq 10$. In particular, by varying the star formation efficiency as a free parameter, we have constrained one of the most unknown parameters of reionization models, the escape fraction f_{esc} of ionizing photons from high-redshift galaxies. The main findings of our work are that, averaged over the galaxy population, (i) the escape fraction shows a moderate increase from $f_{\text{esc}} = 0.068_{-0.047}^{+0.054}$ at $z = 6$ to $f_{\text{esc}} = 0.179_{-0.132}^{+0.331}$ at $z = 8$; (ii) at $z = 10$ we can only put a lower limit of $f_{\text{esc}} > 0.146$. Thus, although errors are large, there is an indication of a 2.6 times increase of the average escape fraction from $z = 6$ to $z = 8$ which might partially release the “starving reionization” problem. At the same time, the best-fit value of the star formation efficiency ϵ_* nominally increases from 3.6% at $z = 6$ to 5.2% at $z = 8$. Such a small variation is statistically consistent with a constant value of ϵ_* , i.e. no evolution.

Parallel to our more phenomenological approach, in the past few years many numerical and analytical studies have attempted to constrain f_{esc} reaching often contradictory conclusions, likely due to uncertainties on star formation history, feedback, radiation transfer and the geometry of the ISM distribution (Fernandez & Shull 2011). Increasing (Razoumov & Sommer-Larsen 2006, 2010; Haardt & Madau 2011), decreasing (Wood & Loeb 2000) or unevolving (Gnedin 2008; Yajima, Choi & Nagamine 2011) trends have been suggested as a function of redshift.

A strong redshift evolution of the escape fraction was recently found by Kuhlen & Faucher-Giguere (2012). They show that, models in which star formation is strongly suppressed in low-mass haloes, can simultaneously satisfy reionization and lower redshift Lyman- α forest constraints only if the escape fraction of ionizing radiation increases from $\sim 4\%$ at $z = 4$ to ~ 1 at higher redshifts. Although broadly in agreement with their conclusions, our results show instead that reionization and LF data can be satisfied simultaneously if f_{esc} grows from $\sim 7\%$ at $z = 6$ to $\sim 18\%$ at $z = 8$, but without requiring an escape fraction of order of unity at these redshifts. We believe that this discrepancy can be understood as due to the fact that unlike Kuhlen & Faucher-Giguere (2012), we are fitting the *full CMB spectrum* rather than the single value of τ_{el} ; the latter choice can be thought as a simplification of CMB polarization observations. In addition, we have used a PCA analysis to optimize model parameters to reionization data, yielding a more robust statistical analysis.

Although here we have only considered the evolution of $z \geq 6$ luminosity functions, our approach can also be applied to model the LFs at $3 \leq z \leq 5$. As hydrogen reionization mostly occurs at $z \gtrsim 6$, the LFs in this lower redshift range are very unlikely to be sensitive to the details of reionization history. Also, dust extinction at $z < 6$ can decrease f_{esc} by absorbing the ionizing photons at these epochs (Yajima, Choi & Nagamine 2011). As a caveat we mention that the present results can be responsive to changes in some cosmological parameters, mainly σ_8 and n_s (Pandolfi et al. 2011). A larger σ_8 or n_s may lead to an increase in the number of collapsed

haloes at all redshifts. In principle then, one should include these two quantities in the analysis as additional free parameters. Also, it could be interesting to evaluate the effects of PopIII stars and other feedback processes in our LF calculation. We hope to revisit some of these topics in more detail in future work.

REFERENCES

Barkana R., Loeb A., 2001, *Phys. Rep.*, 349, 125
 Bergvall N., Zackrisson E., Andersson B. G., Arnberg D., Masegosa J. and Östlin G., 2006, *A&A*, 448, 513
 Bolton J. S., Haehnelt M. G., 2007, *MNRAS*, 382, 325
 Bouwens R., Illingworth G., 2006, *New Astronomy Review*, 50, 152
 Bouwens R. J., Illingworth G. D., Franx M., Ford H., 2007, *ApJ*, 670, 928
 Bouwens R. J., Illingworth G. D., Franx M., Ford H., 2008, *ApJ*, 686, 230
 Bouwens R. J., Illingworth G. D., Franx M., Chary R., Meurer G. R., Conselice C. J., Ford H., Giavalisco M., van Dokkum P., 2009, *ApJ*, 705, 936
 Bouwens R. J., Illingworth G. D., Gonzalez V., Labbe I., Franx M., Conselice C. J., Blakeslee J., van Dokkum P., Ford H., Holden B., Marchesini D., Magee D., Zheng W., 2010, *ArXiv e-prints*
 Bouwens R. J., Illingworth G. D., Oesch P. A., Labbe I., Trenti M., van Dokkum P., Franx M., Stiavelli M., Carollo C. M., Magee D., Gonzalez V., 2010, *ArXiv e-prints*
 Bouwens R. J., Illingworth G. D., Oesch P. A., Stiavelli M., van Dokkum P., Trenti M., Magee D., Labbé I., Franx M., Carollo C. M., Gonzalez V., 2010, *ApJL*, 709, L133
 Bradley L. D., Trenti M., Oesch P. A., Stiavelli M., Treu T., Bouwens R. J., Shull J. M., Holwerda B. W., Pirzkal, N., 2012, *ArXiv e-prints*, 1204.3641
 Bouwens R. J., Illingworth G. D., Oesch P. A., Trenti M., Stiavelli M., Carollo C. M., Franx M., van Dokkum P. G., Labbé I., Magee D., 2010, *ApJL*, 708, L69
 Bruzual G., Charlot S., 2003, *MNRAS*, 344, 1000
 Choudhury T. R., Ferrara A., 2005, *MNRAS*, 361, 577
 Choudhury T. R., Ferrara A., 2006a, in Fabbri R., ed, *Cosmic Polarization. Research Signpost*, p. 205
 Choudhury T. R., Ferrara A., 2006b, *MNRAS*, 371, L55
 Choudhury T. R., Ferrara A., 2007, *MNRAS*, 380, L6
 Choudhury T. R., 2009, *Current Science*, 97, 841
 Ciardi B., Bianchi S., Ferrara A., 2002, *MNRAS*, 331, 463
 Dayal P., Ferrara A., Saro A., Salvaterra R., Borgani S., Tornatore L., 2009, *MNRAS*, 400, 2000
 Dayal P., Ferrara A., Saro A., 2010, *MNRAS*, 402, 1449
 Dijkstra M., Wyithe J. S. B., Haiman Z., 2007, *MNRAS*, 379, 253
 Dove J. B., Shull J. M., Ferrara A., 2000, *ApJ*, 531, 846
 Fan X., Strauss M. A., Becker R. H., White R. L., Gunn J. E., Knapp G. R., Richards G. T., Schneider D. P., Brinkmann J., Fukugita M., 2006, *AJ*, 132, 117
 Faucher-Giguère C., Lidz A., Hernquist L., Zaldarriaga M., 2008a, *ApJ*, 688, 85
 Fernández-Soto A., Lanzetta K. M. and Chen H.-W., 2003, *MNRAS*, 342, 1215
 Fernandez E. R., Shull J. M., 2011, *ApJ*, 731, 20
 Gallerani S., Choudhury T. R., Ferrara A., 2006, *MNRAS*, 370, 1401
 Giallongo E., Cristiani S., D’Odorico S. and Fontana A., 2002, *ApJ*, 568, 9
 Gnedin N. Y., 2008, *ApJ*, 673, 1
 Gnedin N. Y., Kravtsov A. V. and Chen H.-W., 2008, *ApJ*, 672, 765
 Haardt F. and Madau P., 2011, *ArXiv e-prints* 1103.5226
 Heckman T. M., Sembach K. R., Meurer G. R., Leitherer C., Calzetti D. and Martin C. L., 2001, *ApJ*, 558, 56
 Henry A. L., Siana B., Malkan M. A., Ashby M. L. N., Bridge C. R., Chary R., Colbert J. W., Giavalisco M., Teplitz H. I., McCarthy P. J., 2009, *ApJ*, 697, 1128
 Huterer D., Starkman G., 2003, *Physical Review Letters*, 90, 031301
 Iliev I. T., Shapiro P. R., McDonald P., Mellema G., Pen U., 2008, *MNRAS*, 391, 63
 Inoue A. K., Iwata I., Deharveng J.-M., Buat V. and Burgarella D., 2005, *A&A*, 435, 471
 Iye M., Ota K., Kashikawa N., Furusawa H., Hashimoto T., Hattori T., Matsuda Y., Morokuma T., Ouchi M., Shimasaku K., 2006, *Nature*, 443, 186
 Kuhlen, M., & Faucher-Giguere, C. 2012, *ArXiv e-prints* 1201.0757
 Kulkarni, G. and Choudhury, T. R., 2011, *MNRAS*, 412, 2781
 Larson D. et al., 2010, *ArXiv e-prints*, 1001.4635
 Leitherer C., Ferguson H. C., Heckman T. M. and Lowenthal J. D., 1995, *ApJ*, 454, 19
 Loeb A., Barkana R., 2001, *ARA&A*, 39, 19
 McLure R. J., Dunlop J. S., Cirasuolo M., Koekemoer A. M., Sabbi E., Stark D. P., Targett T. A., Ellis R. S., 2010, *MNRAS*, 403, 960
 Miralda-Escudé J., Haehnelt M., Rees M. J., 2000, *ApJ*, 530, 1
 Mitra S., Choudhury T. R., Ferrara A., 2012, *MNRAS*, 419, 1480
 Mitra S., Choudhury T. R., Ferrara A., 2011, *MNRAS*, 413, 1569
 Oesch P. A., Bouwens R. J., Illingworth G. D., Carollo C. M., Franx M., Labbé I., Magee D., Stiavelli M., Trenti M., van Dokkum P. G., 2010, *ApJL*, 709, L16
 Oesch D. et al., 2012, *ApJ*, 745, 110
 Oke J. B., Gunn J. E., 1983, *ApJ*, 266, 713
 Ota K., Iye M., Kashikawa N., Shimasaku K., Kobayashi M., Totani T., Nagashima M., Morokuma T., Furusawa H., Hattori T., Matsuda Y., Hashimoto T., Ouchi M., 2008, *ApJ*, 677, 12
 Pandolfi S., Ferrara A., Choudhury T. R., Melchiorri A., Mitra S., 2011, *Phys. Rev. D*, 84, 123522
 Razoumov A. O. and Sommer-Larsen J., 2010, *ApJ*, 710, 1239
 Razoumov A. O. and Sommer-Larsen J., 2006, *ApJ*, 651, 89
 Samui S., Srianand R., Subramanian K., 2007, *MNRAS*, 377, 285.
 Shapley A. E., Steidel C. C., Pettini M., Adelberger K. L. and Erb D. K., 2006, *ApJ*, 651, 688
 Songaila A., Cowie L. L., 2010, *ApJ*, 721, 1448
 Sbrinovsky J. A., Wyithe J. S. B., 2010, *PASA*, 27, 110
 Taylor J. R., 1997, *An Introduction to Error Analysis: The Study of Uncertainties in Physical Measurements*. University Science Books, 1997, 2nd ed., 327 pages
 Thoul A. A., Weinberg D. H., 1996, *ApJ*, 465, 608
 Vanzella E. et al., 2010, *ApJ*, 725, 1011
 Wood K. and Loeb A., 2000, *ApJ*, 545, 86
 Wyithe J. S. B., Loeb A., 2005, *ApJ*, 625, 1
 Yajima H., Choi J.-H. and Nagamine K., 2011, *MNRAS*, 412, 411